ELSEVIER

Journal of Nuclear Materials 279 (2000) 1–18

journal of nuclear materials

www.elsevier.nl/locate/jnucmat

Review

Thermophysical properties of uranium dioxide

J.K. Fink *

Reactor Engineering Division, Argonne National Laboratory, 9700 South Cass Avenue, Argonne, IL 60439, USA

Received 7 July 1999; accepted 11 November 1999

Abstract

Experimental data on thermodynamic and transport properties of solid and liquid UO_2 have been reviewed and analyzed to obtain consistent equations for the thermophysical properties. Thermodynamic properties that have been assessed include enthalpy, heat capacity, enthalpy of fusion, thermal expansion, density, surface tension and vapor pressure. Transport properties that have been assessed are thermal diffusivity, thermal conductivity, viscosity, emissivity and optical constants. The assessments include a review of the experiments and data, review of previous recommendations, analysis of data to obtain new recommendations, determination of uncertainties in the recommended values, and comparisons of new recommendations with data and previous recommendations. Published by Elsevier Science B.V. All rights reserved.

1. Introduction

Since the last complete open literature assessment by Fink et al. [1] and the assessment reported by Harding et al. [2], there have been sufficient new measurements of thermophysical properties of solid and liquid UO_2 [3–17] and new theoretical research to warrant a complete review of the thermophysical properties. The new measurements are listed in Table 1 according to property. Experimental data [3,4] now confirm the λ-phase transition in the solid, which had been theoretically predicted based on the fluorite structure of UO_2 and on analysis of enthalpy data. Recently, a new microscopic model of this high-temperature phase transition has been developed [18] that includes a self-consistent treatment of point defects and electron interactions with strong screening of the defect charges and provides good agreement with the measured defect concentration [3]. An increased theoretical understanding of UO_2 has led to three phenomenologically based equations for the thermal conductivity of solid UO_2 [5,19,20]. In addition, re-analysis [21] of Argonne National Laboratory's modulated temperature wave measurements of the thermal diffusivity of liquid UO_2 [22] indicated an error in the original analysis of the experiment that results in an error of approximately a factor of two in the reported values for the thermal diffusivity of liquid UO_2. A preliminary review of the thermophysical properties of UO_2 was completed in 1997 [23] and distributed for peer review. This paper includes re-assessments based on peer review comments on that report and new analyses that include the 1999 data of Ronchi et al. [5].

In analysis of these new data and the older existing data, care was taken that the recommendations are consistent. For consistency, enthalpy data and heat capacity data were analyzed together. Thermal diffusivity data were converted to thermal conductivity using the recommended equations for heat capacity and density so that these properties are consistent. Development of new equations to represent the heat capacity and enthalpy of solid UO_2, led to re-examination of the enthalpy of fusion and re-analysis of the liquid enthalpy and heat capacity data to ensure consistency. In the sections below, recommended equations are given for each property. Uncertainties for the recommended properties as functions of temperature are presented in the tables.

2. Enthalpy and heat capacity of solid UO_2

Since the 1981 assessment, significant progress has been made in the understanding of the structure of UO_2

* Tel.: +1-630 252 3182; fax: +1-630 252 3361.
E-mail address: jkfink@anl.gov (J.K. Fink).

PII: S0022-3115(99)00273-1

Table 1
UO_2 property measurements since the 1981 review

Property	Measurements	Reference
λ-transition	Confirmation by neutron scattering	[3]
	Modeled from heat capacity data	[4]
Heat capacity	λ-transition region, 2670–3120 K	[4]
	2000–2900 K	[5]
	3120–8000 K	[6]
Thermal expansion	Lattice parameters, 1060–2900 K	[3]
	$\Delta L/L$, 298–1500 K	[7]
Thermal diffusivity	Solid, 2000–2900 K	[5]
	Liquid, 3130–3275 K	[8]
Thermal conductivity	Liquid, 3473 K, near melting point	[9,10]
Vapor pressure	UO_2 fission heated, in reactor, 3600–6200 K	[11]
	Laser heating, vaporization, 3120–5000 K	[12]
	In reactor, effective equation of state, 3120–7200 K	[13,14]
	Laser heating, boiling point method, 3500–4500 K	[15]
Optical constants	Index of refraction, absorption coefficient, 3100–3600 K	[16,17]

and the contributions to the enthalpy and heat capacity as a function of temperature. The λ-phase transition in solid UO_2 at 2670 K, that had been included in the enthalpy equations recommended by Fink et al. [1,25], was confirmed by Hutchings et al. [3] using neutron scattering experiments to study the oxygen defects and by Hiernaut et al. [4] from the analysis of cooling curves of $UO_{2\pm x}$. Hiernaut et al. [4] reported a λ-phase transition at 2670 ± 30 K in $UO_{2.00}$ and developed a model for the transition as a function of stoichiometry and temperature. From interpretation of these experimental data, Ronchi and Hyland [24] calculated the contributions from each process to compare with available data and provided an excellent description of the theoretical understanding of the contributions from each physical process to the heat capacity. They found that from room temperature to 1000 K, the increase in heat capacity is governed by the harmonic lattice vibrations, which may be approximated by a Debye model. Between 1000 and 1500 K, the heat capacity increase arises from the anharmonicity of the lattice vibrations as evidenced in thermal expansion. The increased heat capacity from 1500 to 2670 K is due to the formation of lattice and electronic defects with the main contribution from Frenkel defects. Above the λ-phase transition, the Frenkel defect concentration becomes saturated and Schottky defects become important.

Recently, Ronchi et al. [5] made simultaneous measurements of the heat capacity and thermal diffusivity from 2000 to 2900 K using 1 and 10 ms laser pulses. Although these measurements lacked the sensitivity required to detect the phase transition peak, they showed that above the λ-phase transition, the heat capacity has a temperature dependence that is similar to that prior to the phase transition. Fig. 1 shows that these high-temperature heat capacity data are inconsistent with the constant heat capacity that was recommended by Fink et al. [1,25] and Harding et al. [2]. Therefore, a combined fit of the enthalpy and heat capacity data [5,26–33], which are listed in Table 2, has been made using a nonlinear weighted χ^2 minimization procedure. Data from each experiment was weighted by the inverse of the square of the standard deviation of that data from a smooth curve through all the data in that temperature range. For the two sets of data of Ronchi et al. [5], the standard deviations from the curve given by Ronchi et al. were used to determine appropriate weights. The temperatures of data obtained prior to 1969 were converted from the 1948 International Practical Temperature Scale (IPTS) to the 1968 IPTS.

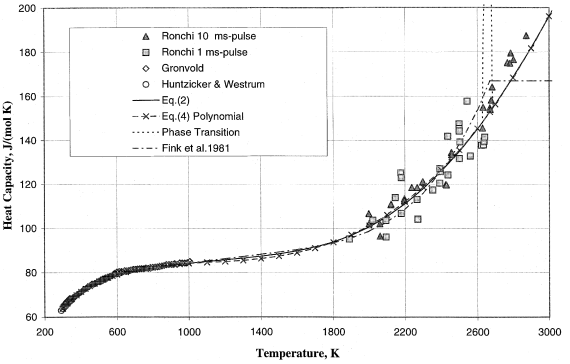

Fig. 1. Solid UO_2 heat capacity data compared with Eq. (2), Eq. (4), and the 1981 equation of Fink et al. [1]. The solid phase transition is indicated by the dashed line.

Table 2
Percent standard deviations of data from the best combined fits of the enthalpy and heat capacity of solid UO_2[a]

Data reference	Temperature range (K)	N	% S.D.	
			Polynomial	Eqs. (1) and (2)
Enthalpy				
[26]	1339–2306	13	3.04	2.25
[27]	483–1464	14	1.80	1.50
[28]	674–1436	24	0.73	0.62
[29,30]	1174–3112	33	0.90	0.86
[31]	2561–3088	12	1.85	1.60
Heat capacity				
[32]	293–346	9	0.72	0.57
[33]	304–1006	88	0.64	0.77
[5]	1997–2873	54	5.96	4.58

[a] N = number of data; % S.D. $= \left[\sum [\{\text{Fit-Data/Data}\} \times 100\%]^2 \Big/ N - \text{free parameters}\right]^{1/2}$.

The heat capacity data of Affortit [34] and Affortit and Marcon [35] were not included in this analysis because of their clear disagreement with other data. The variances (square of the standard deviations) of these data form a smooth curve though all the data are 100 to 1000 times larger than variances of data included in the analysis. Heat capacity data of Popov et al. [36] were excluded because they are high relative to other data. The data of Engel [37] were excluded because they appear to have a systematic error. The variances for the data of Popov et al. and that of Engel are about a factor of 20 higher than the variances for data included in this analysis.

The combined fits of the enthalpy and heat capacity data were constrained by

$$H(T) - H(298.15\ \text{K}) = 0 \text{ at } 298.15\ \text{K}$$

and

$$(\partial H/\partial T)_{\text{P}} = C_{\text{P}},$$

where $H(T) - H(298.15\ \text{K})$ is the enthalpy increment and C_{P} is the heat capacity. Both single equations for the entire temperature range and two equations (one below and one above the transition at 2670 K) were considered. However, the use of two equations did not improve the fits because of inconsistencies between the enthalpy data and the heat capacity data above the λ-phase transition. Fig. 1, which compares the best fits with the heat capacity data, shows that both equations are low relative to the heat capacity data above 2670 K. Comparison of the corresponding enthalpy equations with the enthalpy data in this temperature region, shown in Fig. 2, shows that the enthalpy equations are high relative to the enthalpy data. Use of a second equation above 2670 K that improves the agreement with the heat capacity data, gives poorer agreement with the enthalpy data. Thus, the best fit to the combined enthalpy and heat capacity data is a single equation that is a compromise between the best fit to the high-temperature enthalpy data and the best fit to the high-temperature heat capacity data. Additional data are needed to resolve the apparent inconsistency between the enthalpy data and the heat capacity data above the λ-phase transition.

The values of the variances for the enthalpy data, the heat capacity data, and the combined enthalpy and heat capacity data for the functional forms evaluated are given in Table 3. The smallest total variance was obtained for the 7-term polynomial because it gives the best fit to the low-temperature heat capacity data, which have large weights and a large number of points. However, the functional form containing lattice $+T^2+$ exponential terms fits most data sets better than the polynomial, as shown in Table 2. The best fit to the enthalpy data was with the equation

for $298.15\ \text{K} \leqslant T \leqslant 3120\ \text{K}$

$$\begin{aligned} H(T) - H(298.15\ \text{K}) &= C_1\theta\left[(\mathrm{e}^{\theta/T} - 1)^{-1} - (\mathrm{e}^{\theta/298.15} - 1)^{-1}\right] \\ &\quad + C_2\left[T^2 - (298.15)^2\right] + C_3\mathrm{e}^{-E_a/T}, \end{aligned} \tag{1}$$

where $C_1 = 81.613$

$\theta = 548.68,$

$C_2 = 2.285 \times 10^{-3},$

$C_3 = 2.360 \times 10^{7},$

$E_{\text{a}} = 18531.7,$

T is the temperature in K and the enthalpy increment, $H(T) - H(298.15\ \text{K})$, is in J mol^{-1}.

The temperature derivative of Eq. (1) gives the heat capacity, C_{P}, in J mol^{-1} K^{-1}

for $298.15\ \text{K} \leqslant T \leqslant 3120\ \text{K}$

$$C_P = \frac{C_1\theta^2 e^{\theta/T}}{T^2(e^{\theta/T}-1)^2} + 2C_2T + \frac{C_3E_a e^{-E_a/T}}{T^2}, \quad (2)$$

where the constants are identical to those for Eq. (1). The enthalpy data sets were fit about as well with the 7-term polynomial:

for 298.15 K $\leqslant T \leqslant$ 3120 K

$$H(T) - H(298.15\ \text{K}) = -21.1762 + 52.1743t + 43.9735t^2 - 28.0804t^3 + 7.88552t^4 - 0.52668t^5 + 0.71391t^{-1}, \quad (3)$$

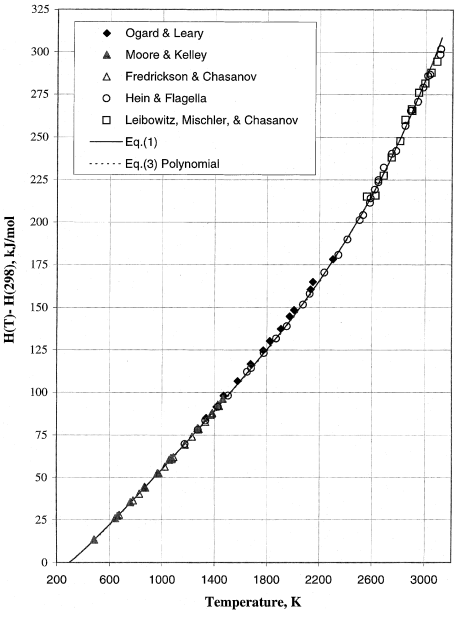

Fig. 2. Comparison of Eqs. (1) and (3) with measurements of the enthalpy increments of solid UO_2.

where $t = T/1000$, T is the temperature in K, and the enthalpy increment, $H(T) - H(298.15\ \text{K})$, is in kJ mol^{-1}. The corresponding heat capacities were calculated from the temperature derivative of Eq. (3), which is

for 298.15 K $\leqslant T \leqslant$ 3120 K

$$C_P(T) = +52.1743 + 87.951t - 84.2411t^2 + 31.542t^3 - 2.6334t^4 - 0.71391t^{-2}, \quad (4)$$

where $t = T/1000$, T is the temperature in K, and the heat capacity, C_P, is in J mol^{-1} K^{-1}.

Fig. 1, which compares the heat capacity data with values calculated from Eqs. (2) and (4), shows that the values obtained from these two equations are almost identical. They deviate by at most 1%, which is less than the scatter in the data. The enthalpy values from these two fits agree within 0.5% and cannot be distinguished in the graph in Fig. 2, which compares these fits with the enthalpy data. Because the fits by both functional forms are almost identical, both equations are recommended. Browning [38] has commented that the ability to calculate the contributions to the heat capacity from each physical process from first principles [24,38] makes analysis of the experimental data using functional forms that approximate some but not all the physical processes obsolete because the constants determined from these fitting procedures are only approximations to the physical parameters. For example, $\theta = 549$ K approximates the Einstein temperature, which is 542 K [38]. Nevertheless, calculations of the contributions of all physical processes from first principles [24,38] are too complicated for practical use. Browning [38] admits that functional forms that approximate physical processes provide a better fit to the experimental data than do fits using polynomials. Because polynomial forms are simpler for inclusion in large computer codes that are used in reactor-safety calculations, the polynomials given in Eqs. (3) and (4) may be preferred.

Table 3
Variances, σ^2, of weighted fits for different equation forms[a]

Enthalpy functional form	# of parameters	Total σ^2	$H\sigma^2$	$C_P\sigma^2$
Lattice $+T^2+$ exponential, Eq. (1)	5	0.34	0.25	0.47
Polynomial, Eq. (3)	7	0.32	0.28	0.38
Lattice $+T^2 + T$ exponential	5	0.55	0.40	0.73
$T < 2670$ K: lattice$+T^2+$exponential $T > 2670$ K: quadratic	8	0.36	0.31	0.38
$T < 2670$ K: lattice + T^2 + exponential $T > 2670$ K: quadratic + exponential	10	0.35	0.29	0.45

[a] $\sigma^2 = \left\{\frac{1}{N-\text{free}}\sum\frac{1}{\sigma_i^2}[y_i - y(T_i)]^2\right\} \Big/ \left\{\frac{1}{N}\sum\frac{1}{\sigma_i^2}\right\}$, where $N =$ number of data, free $=$ # of free parameters, $(1/\sigma_i)^2 =$ weight, $y_i =$ datum, $y(T_i) =$ fit at temperature T_i; Lattice $= C_1\theta/(e^{\theta/T}-1)$, where C_1, and θ are parameters.

3. Enthalpy and heat capacity of liquid UO_2

The recommended equations for the enthalpy and heat capacity of liquid UO_2 are a least-squares fit to the enthalpy data from 3173 to 3523 K of Leibowitz et al. [29,30], the enthalpy data from 3123 to 3260 K of Hein and Flagella [28] and the heat capacity data from 3120 to 4500 K of Ronchi et al. [6]. Although Ronchi et al. made measurements from 3100 to 8000 K, the data fit was limited to the temperature range of 3120–4500 K because this is the range of interest for reactor-safety calculations and the uncertainties in the determined heat capacities increase significantly with temperature above 4500 K. The form of equation used to fit these data is that suggested by Ronchi et al. [6]. The data have been weighted by the inverse of the square of their experimental uncertainties. The enthalpy data were considered to be of higher quality than the heat capacity data because enthalpy values from the two independent measurements are in excellent agreement, the enthalpy increment measurements were done using standard techniques with calibration standards, and the stoichiometry change in these enthalpy experiments were within the variation for reactor fuel. The uncertainty used for all the enthalpy data was 2%. Ronchi et al. [6] state that the uncertainty in the heat capacity data is on the order of 15–20% from 3100 to 5000 K. A 15% uncertainty has been assumed in determining the weight for the heat capacity data.

For the temperature range 3120–4500 K, the recommended equation for the enthalpy increment of liquid UO_2, $H(l,T) - H(s, 298.15\ \mathrm{K})$, in J mol^{-1} is

$$H(l,T) - H(s, 298.15\ \mathrm{K}).$$
$$= 8.0383 \times 10^5 + 0.25136T - \frac{1.3288 \times 10^9}{T}. \quad (5)$$

The heat capacity at constant pressure is the temperature derivative of the enthalpy. For 3120–4500 K, the recommended equation for the heat capacity, C_P, in J mol^{-1} K^{-1} is

$$C_P = +0.25136 + \frac{1.3288 \times 10^9}{T^2}. \quad (6)$$

In Eqs. (5) and (6), the temperature, T, is in K. These equations differ from the equations derived by Fink in the preliminary report ANL/RE-97/2 [23], which were constrained to reproduce the value of the enthalpy at 3120 K given by Rand et al. [39] and thereby preserve the enthalpy change on melting that had been given by Rand et al. Removal of that constraint changed only the coefficient of the second term of Eq. (5), which is also the first term of Eq. (6). Enthalpy values calculated with Eq. (5) differ by 0.3% from those in the preliminary report. The constraint is no longer appropriate because the enthalpy increment of the solid at the melting point calculated from Eq. (3) differs from the value given by Rand et al. [39] and therefore requires new evaluation of the enthalpy of fusion. Figs. 3 and 4 show these recommended equations and the data fit.

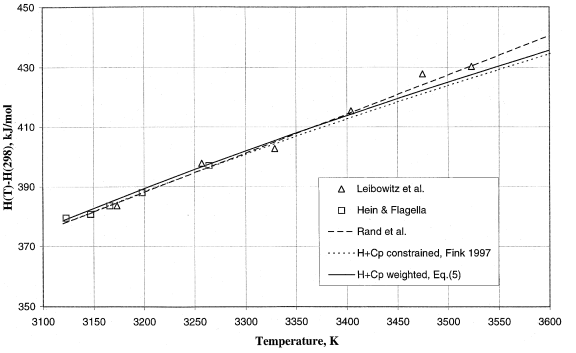

Fig. 3. Equations for the enthalpy increments of liquid UO_2 compared with the available data.

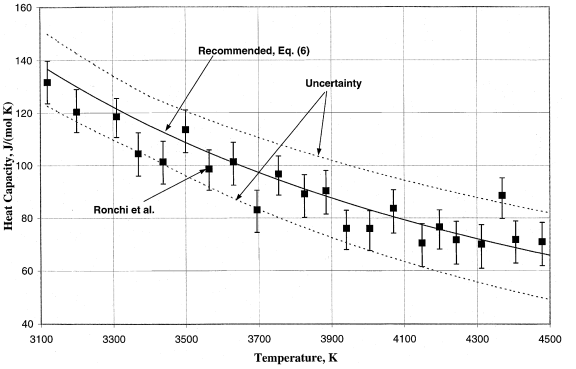

Fig. 4. Comparison of the recommended equation for the heat capacity of liquid UO_2 with the data of Ronchi et al. [6].

4. Enthalpy of fusion

The enthalpy of fusion of UO_2 at 3120 K is 70 ± 4 kJ mol^{-1}, the difference between the enthalpy increment of the liquid at 3120 K, as given by Eq. (5) and the enthalpy increment of the solid at 3120 K, as given by Eq. (3). This recommended value differs by 4.8 kJ mol^{-1} from the value (74.8 kJ mol^{-1}) recommended in the 1981 review by Fink et al. [1] and in the 1989 review by Harding et al. [2]. These two values are both within the uncertainty in the experimental data. The recommended value for the enthalpy of fusion has been changed for consistency with the new equations for solid and liquid enthalpy, which were obtained from combined analysis of enthalpy and heat capacity data. The previous value was

based on analysis of only enthalpy data near the melting point.

5. Thermal expansion and density of solid UO_2

Martin [40] reviewed 15 sets of UO_2 thermal expansion data obtained from lattice parameter measurements and macroscopic length changes. After correcting macroscopic length data that exhibited a zero error, he compared the data and excluded data that disagreed with the common consensus. Because the data of Christensen [41] show significant scatter and disagreed with the very precise lattice data of Hutchings [3], which agree well with the data of Conway [42], Martin excluded the Christensen data from his analysis. The only new data, which have been published since this thorough analysis by Martin, are the data of Momin et al. [7].

The analysis of Martin [40] has been re-examined because it excluded the data of Christensen [41], which are still being used in determining density equations [5] and the recent data of Momin et al. [7] fall outside the errors given by Martin. A weighted least-squares minimization procedure has been used to fit the thermal expansion data [3,42–49] that were fit by Martin, the data of Christensen [41], and the data of Momin et al. [7]. The weights used for the data fit by Martin and the data of Momin et al. are the inverse of the squares of the standard deviations from the equations recommended by Martin. The deviation of the data of Christensen near 1700 K from the common data was used to weight the data of Christensen. The least-squares fit to these data gave equations that differed from those given by Martin by less than 1%. Thus, the equations given by Martin are consistent with this larger data set and are therefore recommended. These equations for the linear thermal expansion of solid UO_2 are

for 273 K $\leqslant T \leqslant$ 923 K

$$L_T = L_{273}\ (9.973 \times 10^{-1} + 9.082 \times 10^{-6} T - 2.705 \times 10^{-10} T^2 + 4.391 \times 10^{-13} T^3) \quad (7)$$

for 923 K $\leqslant T \leqslant$ 3120 K

$$L = L_{273}\ (9.9672 \times 10^{-1} + 1.179 \times 10^{-5} T - 2.429 \times 10^{-9} T^2 + 1.219 \times 10^{-12} T^3), \quad (8)$$

where L and L_{273} are the lengths at temperatures T (in K) and 273 K, respectively. The fractional change in length of UO_2, $\Delta L/L = (L - L_{273})/L_{273}$, expressed as a percent, is shown in Fig. 5 with the recommended uncertainties and the data fit. The recommended uncertainties shown in Fig. 5 have been increased from those given by Martin in order to include most of the data by Momin et al. and some of the high-temperature data of Christensen [41] and Baldcock [43].

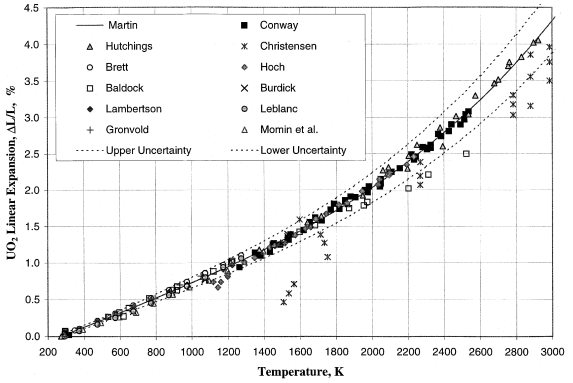

Fig. 5. Measurements of the linear expansion, $\Delta L/L$, of solid UO_2 compared with the recommended equation of Martin [40] and its recommended uncertainties.

The cubic polynomials given by Martin for the instantaneous linear thermal expansion coefficients, α_P (l), are recommended. These equations do not differ by more than 0.6% from the exact partial differentials that are defined as

$$\alpha_P(l) = \frac{1}{L}\left(\frac{\partial L}{\partial T}\right)_P. \quad (9)$$

For 273 K $\leqslant T \leqslant$ 923 K,

$$\alpha_P(l) = 9.828 \times 10^{-6} - 6.930 \times 10^{-10} T + 1.330 \times 10^{-12} T^2 - 1.757 \times 10^{-17} T^3; \quad (10)$$

for 923 K $\leqslant T \leqslant$ 3120 K

$$\alpha_P(l) = 1.1833 \times 10^{-5} - 5.013 \times 10^{-9} T + 3.756 \times 10^{-12} T^2 - 6.125 \times 10^{-17} T^3, \quad (11)$$

where $\alpha_P(l)$ is the coefficient of thermal expansion in K^{-1} and temperature, T, is in K.

The density of solid UO_2 as a function of temperature may be calculated from

$$\rho(T) = \rho(273)\left(\frac{L_{273}}{L_T}\right)^3, \quad (12)$$

where ρ (273) is the density at 273 K = 10.963 Mg m^{-3}. The ratio L_{273}/L_T as a function of temperature is given by Eqs. (7) and (8). The recommended densities are identical to those given by Harding et al. [2]. Between 298 and 2500 K, densities calculated using these equations are within 0.5% of the values recommended by Fink et al. [1] and the values given by the equation of Ronchi et al. [5]. At temperatures above 2500 K, they are within 1% of the values given by Fink et al. and within 1.7% of those of Ronchi et al.

6. Thermal expansion and density of liquid UO_2

The recommended equation for the thermal expansion coefficient of liquid uranium dioxide is based on the in-pile measurements from 3120 to 7600 K on UO_2 and (U, Pu)O_2 by Breitung and Reil [50]. The equation given by Breitung and Reil for the thermal expansion coefficient of UO_2 and (U, Pu)O_2 for mole fractions of Pu $\leqslant 0.25$ is in good agreement with the equation for the thermal expansion coefficient of UO_2 from experiments by Drotning [51], which had been recommended in the 1981 assessment by Fink et al. [1] The recommended equation for the instantaneous volumetric thermal expansion coefficient of UO_2 as a function of temperature is

$$\alpha_P(l) = \frac{0.9285}{8860 - 0.9285(T - 3120)}, \tag{13}$$

where $\alpha_P(l)$ is the coefficient of thermal expansion in K^{-1} and temperature, T, is in K.

The recommended equation for the density of liquid UO_2 is the equation given by Breitung and Reil [50], which is consistent with the recommended liquid coefficient of thermal expansion

$$\rho = 8.860 - 9.285 \times 10^{-4}(T - 3120), \tag{14}$$

where density, ρ, is in Mg m^{-3} and temperature, T, is in K. In Fig. 6, the recommended density equation is compared with data of Drotning [51] and of Christensen [41], and with equations of Christensen and Harding et al. [2]. The equation of Drotning [51], which had been recommended by Fink et al. [1], is not shown in Fig. 6 because it cannot be distinguished from the recommended equation of Breitung and Reil, Eq. (14). Although the equation of Harding et al. [2] has the same slope as the recommended equation, these equations differ by the density at the melting point. The recommended density at the melting point, 8.86 Mg m^{-3}, is the melting point density given by Drotning [51], which was also recommended by Fink et al. [1]. The melting point density recommended by Harding et al. was calculated using the solid density given by the equation of Martin [2] and the change of density on melting determined by Christensen [41]. Because the measurements by Drotning are more precise than those of Christensen and because the solid thermal expansion data of Christensen are not in good agreement with the precise data of Hutchings [3], the melting point density of Drotning is recommended rather than the change in density on melting of Christensen.

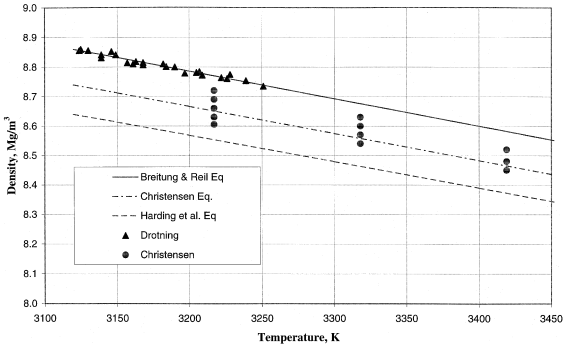

Fig. 6. Comparison of the data of Drotning [51] and of Christensen [41] with equations for the density of liquid UO_2.

7. Thermal diffusivity and thermal conductivity of solid UO_2

Data for the thermal diffusivity [5,52–56] and thermal conductivity [56–58] of solid UO_2 have been re-assessed for the following reasons. (1) Advances in understanding the heat transport mechanisms in UO_2 has led to improvements in physically based thermal conductivity equations [5,19,20] so that the few parameters that are determined from fitting the thermal conductivity data are the coefficients of the phonon lattice contribution. (2) Thermal conductivities calculated from thermal diffusivity data using heat capacities given by Eq. (4), which is based on the recent measurements of Ronchi et al. [5], have a different temperature dependence from the older values. (3) The 2000–2900 K thermal diffusivity data of Ronchi et al. [5] indicate that the high-temperature thermal diffusivity values reported by Weilbacher [52,53], which were the main high-temperature data available prior to 1999, are high. Data included in this re-assessment are listed in Table 4, which also gives the percent of theoretical density of the samples, the temperature range of the measurements, and the number of data obtained for each set of measurements. Although Conway and Feith [56] report results of the General Electric (GE) Nuclear Systems Programs (NSP) thermal diffusivity measurements from 600 to 1700 K as well as data from the GE-NSP 'round robin' thermal conductivity measurements, only the thermal conductivity data have been included in this assessment because comparison of the thermal diffusivity data with other data show large disagreement above 1200 K. Temperatures for the data of Stora et al. [58] and Godfrey et al. [57] have been converted from the 1948 IPTS to the 1968 IPTS.

The differences between the thermal diffusivity values of Weilbacher and Ronchi et al. are clearly shown in Fig. 7, which plots the inverse of the measured thermal diffusivities as a function of temperature. The percent of theoretical density of the samples for each set of measurements has been included in the figure legend. From 300 to 2000 K, all the inverse thermal diffusivity data show a linear dependence on temperature. Although the data of Hobson et al. [54] and Ronchi et al. [5] continue to increase linearly with temperature to 2400 K, values

Table 4
Standard deviations of data from recommended thermal conductivity equation

Data reference	Percent of theoretical density (%)	Temperature range (K)	# of data	S.D. (%)	
				Ronchi Eq. (16)	Recommended Eq. (19)
Thermal diffusivity measurements					
[5]	95	550–1100 2000–2900	125	8.6	7.2
[54]	95	537–2488	34	8.0	3.6
Weilbacher (two runs) [52,53]	98	773–3023	32	7.1	11.4
Bates (three samples) [55]	98.4	289–2777	188	8.7	6.0
[56]	97.4	457–2271	27	6.8	4.2
[56]	98	299–2083	35	9.7	12.4
Thermal conductivity measurements					
GE Nuclear Systems Programs, 1969 [56]	98	1229–2661	70	5.9	8.0
Centre d'Etudes Nucleaires (CEN) Grenoble, 1969 [56]	97	373–2577	14	8.0	10.6
[57]	93.4	323–1573	105	7.5	3.7
[58]	95	473–2777	19	8.4	10.9

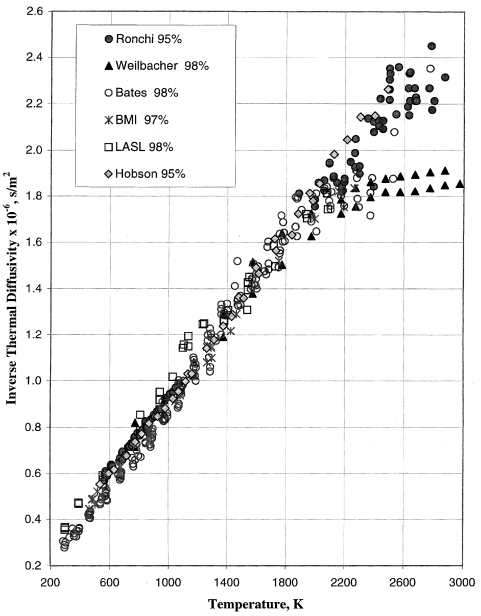

Fig. 7. The inverse of measured thermal diffusivities as a function of temperature.

from the measurements of Weilbacher deviate from the linear dependence above 2000 K. Ronchi et al. [5] attribute the high diffusivity values obtained by Weilbacher [52,53] to incorrect determinations of the temperature rise of the front of the sample and to errors in the Cowan correction during data reduction. Measurements of Bates [55] on three different samples span almost the entire temperature range but show considerable scatter. At low temperatures, values of the inverse thermal diffusivity from Bates measurements are below the values of Ronchi et al. [5]. Between 2000 and 2400 K, Bates' values [55] fall between Weilbacher's values [52,53] and those of Ronchi et al. [5]. However, the highest temperature datum of Bates [55] is consistent with the data of Ronchi et al. [5].

Since 1981, theoretical research and new measurements have led to improvements in equations for the thermal conductivity of UO_2. The physically based equation of Hyland [19] included phonon lattice, radiation, and a small polaron ambipolar contributions. The equation of Hardin and Martin [20] consisted of a phonon lattice term and a small polaron ambipolar contribution. Since the publication of these equations, Casado et al. [59] have shown that the temperature dependence used by Killeen [60] in analysis of his electrical conductivity data is incorrect. This temperature dependence had been incorporated in the small polaron ambipolar contribution in the thermal conductivity equations of Hyland [19], and Harding and Martin [20]. Casado et al. [59] reported that the correct temperature dependence for the small polaron contribution to the direct current electrical conductivity, $\sigma(T)$, is

$$\sigma(T) = \frac{\sigma_1}{T^{3/2}} e^{-\varepsilon/kT}, \tag{15}$$

where ε is the activation energy in eV of the direct current electrical conductivity, σ_1, k is the Boltzmann constant and T is the temperature. Ronchi et al. [5] used this

temperature dependence to refit the electrical conductivity data of Killeen [60] and determined a new term for the ambipolar contribution to the thermal conductivity of UO_2. They extracted a phonon lattice contribution by fitting the thermal resistivities obtained from their diffusivity measurements from 550 to 1100 K. The equation given by Ronchi et al. for the thermal conductivity of 95% dense UO_2 is

$$\lambda = \frac{100}{6.548 + 23.533t} + \frac{6400}{t^{5/2}} \exp\left(\frac{-16.35}{t}\right), \tag{16}$$

where $t = T$ (K)/1000, and λ is the thermal conductivity for 95% dense UO_2 in W m^{-1} K^{-1}.

Ronchi et al. [5] also fit their data to a polynomial. In Fig. 8, these two equations of Ronchi et al. are compared with the data listed in Table 4 converted to thermal conductivity for 95% dense UO_2. Thermal conductivities have been calculated from thermal diffusivity measurements [52–56] using the relationship

$$\lambda = D\rho C_P, \tag{17}$$

where λ is the thermal conductivity, D the measured thermal diffusivity, ρ the sample density calculated using Eqs. (7) (8) and (12) and the fraction of theoretical density, and C_P the heat capacity given by Eq. (4). For the thermal diffusivity measurements of Ronchi et al. [5], the values of the thermal conductivities tabulated in their paper have been used in this evaluation because these values obtained from the simultaneous measurements of thermal diffusivity and heat capacity have a higher degree of confidence than values obtained using an equation that fits the heat capacity data but does not exactly reproduce experimental values at any given temperature. All thermal conductivities were converted to 95% theoretically dense UO_2 using the equation recommended by Brandt and Neuer [61], which is

$$\lambda_0 = \frac{\lambda_p}{[1 - \alpha p]}, \quad \alpha = 2.6 - 0.5t, \tag{18}$$

where p is the porosity fraction, λ_p the thermal conductivity of UO_2 with porosity p, λ_0 is the thermal conductivity of fully dense UO_2 (i.e., porosity = 0) and $t = T(K)/1000$.

Fig. 8 shows that the high-temperature thermal conductivities of Stora and the 'round robin' Grenoble data are high compared to the equation suggested by Ronchi et al. [5]. These thermal conductivity data were obtained by the radial heat flow method. Ronchi et al., question the reliablity of the high-temperature data of Stora because of vaporization of the sample and mechanical deformations above 2500 K. The GE-NSP data from 2625 to 2657 K show significant scatter. Conway and Feith [56] state that these data should be treated with caution because examination of the GE–NSP samples following high-temperature radial heat flow measurements showed evaporation from the center of the disc and deposition of condensed material along the cooler edges. These questionable data are consistent or higher than the thermal conductivities obtained from the thermal diffusivity measurements of Weilbacher.

Comparison of Eq. (16) with the data shows that, although it appears low relative to the lowest temperature data, it is high relative to the minimum near 2000 K. This might be attributed to the linear temperature dependence of the lattice phonon term, which includes only constant volume three phonon scattering processes. Ronchi et al., state that they considered including a T^2 term in their fit to their low temperature data to account for constant pressure thermal expansion contributions but the additional term was not statistically justified. In an attempt to improve agreement at low temperatures (below 550 K) and in the region of the thermal conductivity minimum, the phonon lattice contribution has been re-examined. Because the data of Weilbacher, the data of Stora, the Grenoble data and the GE–NSP data above 2600 K are questionable, these sets of data have been excluded from this analysis. The phonon lattice contribution for each thermal conductivity datum has been calculated by subtracting the small polaron ambipolar contribution, given by the second term of Eq. (16), from each thermal conductivity datum. In fitting the inverse of the phonon lattice contribution, both linear and quadratic temperature terms have been considered. T tests of goodness of fit indicate that a quadratic term is justified. The recommended equation for the thermal conductivity of 95% dense UO_2 includes this new phonon lattice term and the small polaron ambipolar contribution determined by Ronchi et al. [5]. It is

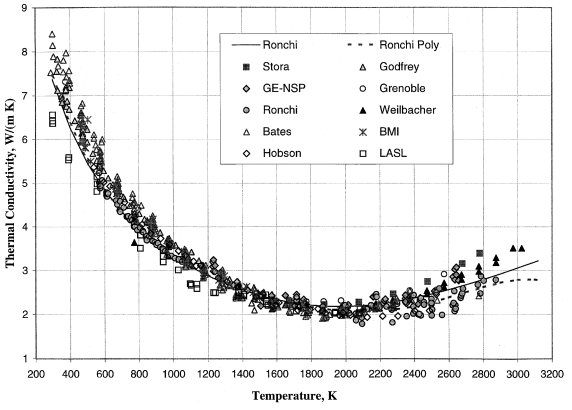

Fig. 8. Comparison of data for 95% dense UO_2 from thermal conductivity and thermal diffusivity measurements with the equations of Ronchi et al. [5], (Eq. (16) in this paper, and their polynomial fit to their data).

$$\lambda = \frac{100}{7.5408 + 17.692t + 3.6142t^2} + \frac{6400}{t^{5/2}} \exp\left(\frac{-16.35}{t}\right), \tag{19}$$

where $t = T$ (K)/1000, and λ is the thermal conductivity of 95% dense UO_2 in W m^{-1} K^{-1}. This equation fits the data of Ronchi et al., Bates, Hobson et al., Godfrey et al., and the 'round robin' data from BMI, LASL, and GE-NSP below 2600 K with a percent standard deviation of 6.2%. The standard deviation of these data from the equation given by Ronchi et al., Eq. (16), is 7.9%. Table 4 shows the percent standard deviations from Eqs. (19) and (16), the equation of Ronchi et al., for each set of data. Fig. 9 shows the data fit, the recommended equation, Eq. (19), the equation of Ronchi et al., Eq. (16), and the polynomial fit by Ronchi et al. to their data. At intermediate and high temperatures, the recommended equation is very similar to the polynomial fit to the data of Ronchi et al. The recommended equation fits the data near the thermal conductivity minimum and the low-temperature data of Bates better than Eq. (16).

From their research, Ronchi et al. concluded that the solid thermal conductivity of 95% dense UO_2 at the melting point, T_m, should be in the range $2.4 \leqslant \lambda(T_m) \leqslant 3.1$ W m^{-1} K^{-1}. The thermal conductivity for 95% dense UO_2 at 3120 K calculated with the recommended equation, Eq. (19), is 3.0 W m^{-1} K^{-1} , which is consistent with the conclusion of Ronchi et al.

Historically, the paucity of high-temperature thermal conductivity data prompted the practice of comparing thermal conductivity equations to the in-reactor conductivity integral to melt (CIM) defined as

$$\mathrm{CIM} = \int_{773\ \mathrm{K}}^{T_m} \lambda(T)\, \mathrm{d}T, \tag{20}$$

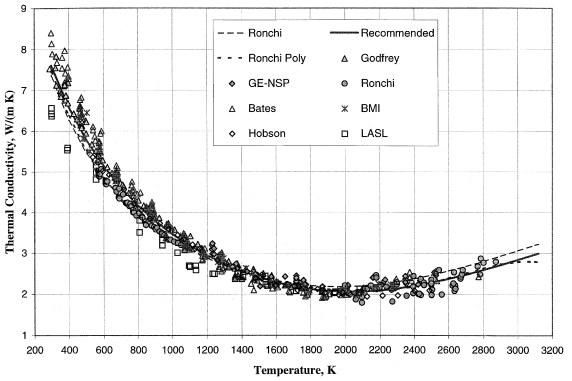

Fig. 9. Comparison of the recommended equation for the thermal conductivity of 95% dense UO_2, Eq. (19) with the data fit and the equations of Ronchi et al. [5] (physically based Eq. (16) and polynomial fit to their measurements).

where $\lambda(T)$ is the thermal conductivity at temperature T and T_m is the melting point. This integral represents the reactor linear power at which melting begins on the centerline of a fuel pellet whose outer surface is assumed to be at 773 K. The CIM obtained from the recommended equation, Eq. (19), is 6.09 kW m^{-1}. The polynomial used by Ronchi et al. to fit their data gives a CIM of 6.08 kW m^{-1}. Experimental values for CIM range from 5.5 to 7.5 kW m^{-1}. Because in-reactor CIM measurements are subject to systematic errors such as determination of the pellet surface temperature from the cladding temperature and the fuel–cladding gap conductance, and considerable controversy exists in the interpretation of the melt boundary from the post-test metallurgical examinations, the CIM value is still uncertain. However, CIM values near 6.8 kW m^{-1} have been recommended for 95% dense fuel [62]. These values were consistent with equations [19,20] used to fit the high-temperature thermal conductivity of Weilbacher. Ronchi et al. [5] state that although the most complete set of measurements at GE-San Jose' gave 6.3 ± 0.3 kW m^{-1} [63] for CIM, these results were not accepted because they were below values based on laboratory determinations. The GE values and the previous recommendations should be re-considered now that more reliable laboratory data are available at high temperatures.

8. Thermal conductivity and thermal diffusivity of liquid UO_2

In 1994, Ronchi [64] reviewed the available data [8–10,22] and analyses [19,21] on the thermal conductivity and thermal diffusivity of solid and molten UO_2 near the melting point and recommended a thermal conductivity of 2.5 ± 1 W m^{-1} K^{-1} for liquid UO_2 at the melting point based on the requirement that the thermal diffusivity should be continuous across the melting point. The value for the thermal conductivity of molten UO_2 that was recommended by Ronchi is recommended here but the basis for the recommendation differs somewhat because of new data available since 1994.

Ronchi stated that materials that have an order/disorder transition near the melting point, such as the transition at 2670 K in UO_2, have a thermal diffusivity that increases continuously across the melting point because the change in slope of the thermal diffusivity occurs at the order/disorder transition rather than at the melting point. Above the order/disorder transition, these materials exhibit glassy behavior. From the solid thermal conductivity at the melting point that is obtained from the equation of Hyland [19], 3.65 W m^{-1} K^{-1}, Ronchi calculated that the solid thermal diffusivity at the melting point is in the range of $6.2–6.7 \times 10^{-7}$ m^2 s^{-1}. These values give good agreement with the value

6.4×10^{-7} m^2 s^{-1} that he calculated from Tasman's thermal conductivity measurement [10], 2.5 W m^{-1} K^{-1}, and the melting point heat capacity measured by Ronchi et al., using Tasman's thermal conductivity value in the data reduction.

The recent simultaneous thermal diffusivity and heat capacity measurements of Ronchi et al. [5] give a thermal diffusivity at the melting point of 4.2×10^{-7} m^2 s^{-1} and show no discontinuity around 2670 K. The lack of discontinuity may be due to the lack of sensitivity in these measurements, which were unable to detect the discontinuity in the heat capacity at 2670 K. Not only is this value for the thermal diffusivity at the melting point lower than the value obtained from the thermal conductivity of Tasman, it is significantly lower than values from thermal diffusivity measurements of Otter and Damien [8] and Kim et al. [22]. In 1985, Fink and Leibowitz [21] re-analyzed the thermal diffusivity measurements of Kim et al. and concluded that: (1) there was an error of approximately a factor of 2 in the ideal model used by Kim et al. (2) if the thermal conductivity was low, then the ideal model used by Kim et al. was not valid because the conductivity of the tungsten wall becomes important and (3) there was a statistically significant difference between the thermal conductivities of the thick and thin layers. The difference between the thin and thick cell results is analogous to differences observed in thermal diffusivity measurements of glassy and liquid materials in which radiation is important and cannot be neglected [65,66]. Ronchi's statement that, above the solid phase transition at 2670 K, UO_2 exhibits glassy behavior is consistent with the systematic differences in results from thick and thin cells without taking into account radiation. If the assumption is made that the difference in thermal diffusivities between the thick and thin layers of UO_2 in the experiment of Kim et al., arises from the failure to include the radiative term in the analysis and the radiative contribution scales according to the thickness of the UO_2 layer, the experimental thermal diffusivity of a 0.2 mm thickness of UO_2 (thickness of the molten layer in the experiment of Tasman) can be estimated. For the temperatures of 3250 and 3277 K, this estimate gives thermal diffusivities of 5.8×10^{-7} and 6.7×10^{-7} m^2 s^{-1}. These values are consistent with the thermal diffusivity obtained from the thermal conductivity measurements of Tasman.

9. Total vapor pressure over liquid UO_2

The recommended equation for the total vapor pressure over liquid UO_2 from the melting point (3120 K) to 8000 K is the equation derived by Breitung and Reil [67] from their in-pile equation-of-state measurements [13,14] and their review of experimental data from pressure–temperature measurements and pressure–enthalpy measurements. Their equation for the logarithm of the saturated vapor pressure over liquid UO_2 is

$$\log_{10} P = 15.961 - \frac{26\,974}{T} - 2.7600 \log_{10} T, \qquad (21)$$

where the pressure is in MPa and the temperature is in K. This equation gives a boiling point of 3815.1 K.

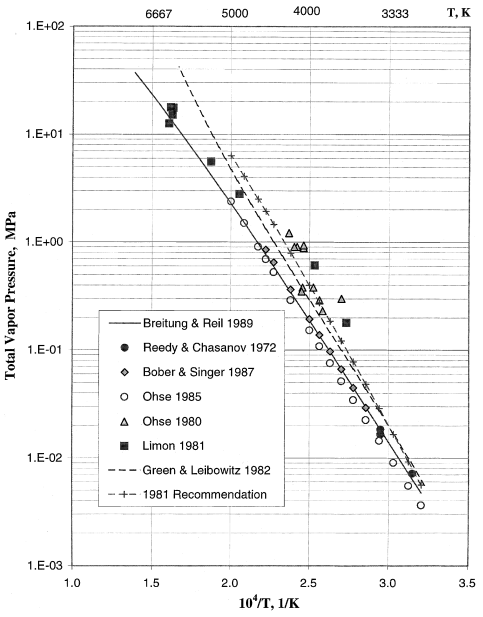

Fig. 10. Equations and data for the total vapor pressure over liquid UO_2 as a function of inverse temperature.

In Fig. 10, vapor pressures calculated with the recommended equation are compared with the most recent and reliable vapor pressure data from each experimental method, with the equation formulated by the 1978 IAEA International Working Group on Fast Reactors and recommended in the 1981 review [1], and with vapor pressures calculated by Green and Leibowitz [68] from spectrocopic data using statistical mechanics and an oxygen potential model. At 4220 K, the 1980 data of Ohse et al. [69] are a factor of 3.3 higher than Eq. (21). The recommended equation of Breitung and Reil is in good agreement with the vapor pressures determined from laser-vaporization experiments in 1985 by Ohse et al. [12] with the low-temperature transpiration data of Reedy and Chasanov [70], with the high-temperature data of Limon et al. [11], and with the boiling-point data of Bober and Singer [15]. It is a good representation of all equilibrium in-pile and out-of-pile data.

10. Enthalpy of vaporization

Breitung and Reil [67] noted that except for the two low-temperature data points of Limon et al., all in-pile

results are located close to a linear extension of the transpiration data of Reedy and Chasanov and the boiling-point data of Bober and Singer. All these methods provide conditions very close to equilibrium vaporization so that the slope of the line connecting these data should give the heat of vaporization. They attributed the steeper slopes obtained from the earlier laser-vaporization experiments (as characterized in Fig. 10 by the 1980 data of Ohse et al. [69]) to the use of nonequilibrium pressure models to reduce the data and/or to the neglect of optical absorption of thermal surface radiation in the vapor cloud. From application of the Clausius–Clapeyron equation to their vapor pressure equation, Breitung and Reil recommend the effective heat of vaporization

$$\Delta H_{\text{vap}} = 516\,382 - 22.946T, \tag{22}$$

where ΔH_{vap} is in J mol^{-1} and T in K ranges from 3120 to 8000 K.

11. Surface tension and surface energy

In 1987, Hall et al. [71–73] completed a critical review of available data on the surface tension of liquid UO_2 and on the surface energy of solid UO_2. Because no new data have been reported since this review, the results of this critical review are recommended. The recommended surface tension of liquid UO_2 at the melting point is the average of measurements by Schins [74], Christensen [75] and Bates [76]. Because no data are available at higher temperatures, the theoretical equation derived by Nikopoulos and Schulz [77] is recommended. It is

$$\gamma_{\text{LV}} = 0.513 - 0.19 \times 10^{-3}\ (T - 3120), \tag{23}$$

where the surface tension, γ_{LV}, is in J m^{-2} and temperature, T, is in K.

From the review of the multi-phase equilibrium measurements of the surface energy of UO_2, Hall et al. [71,72] concluded that from 273 to 3120 K the surface energy (γ_{SV}) in J m^{-2} of solid $UO_{2.00}$ probably lies between the two lines:

$$\begin{aligned}\gamma_{\text{SV}} &= 1.5 - 2.82 \times 10^{-4}(T - 273),\\ \gamma_{\text{SV}} &= 0.20\end{aligned} \tag{24}$$

with the mean line between these given by

$$\gamma_{\text{SV}} = 0.85 - 1.40 \times 10^{-4}(T - 273), \tag{25}$$

where temperature, T, is in K. Hall et al. [71,73] give the dependence of the solid surface energy on stoichiometry as

$$(\gamma_{\text{SV}})_x - \gamma_{\text{SV}} = 6.8x \quad (0 \leqslant x \leqslant 0.05;\ 0 < T < 2170\ \text{K}), \tag{26}$$

where $(\gamma_{\text{SV}})_x$ is the surface energy of $UO_{2\pm x}$ in J m^{-2}. Hall et al. [71] concluded that the effective surface energy for pores in UO_2, γ_{P}, is different from γ_{SV}. It is given by

$$\gamma_{\text{P}} = 0.41\gamma_{\text{SV}}. \tag{27}$$

12. Viscosity

The recommendation for the viscosity of molten UO_2 is identical to that made in the 1981 review [1] because no new measurements are available. Viscosities of liquid uranium dioxide have been measured in the temperature range of 3143–3303 K by Woodley [78], at the melting point (3120 K) by Palinski [79], and from 3083 to 3328 K by Tsai and Olander [80]. The recommended equation is that of Woodley because of the greater precision of his data and the agreement between Woodley and Palinski. The Woodley equation is

$$\eta = 0.988\ \exp\left(\frac{4620}{T}\right), \tag{28}$$

where the kinematic viscosity, η, is in centipoise (mPa s) and T is in K.

13. Emissivity and optical constants

The experiments of Bober et al. [16,17,81,82] for the emissivity, reflectivity and optical constants of UO_2 in the solid and liquid phases provide the most reliable data for these properties. Within the limits of experimental error, the data of Bober et al. [81] for solid UO_2 agree with earlier emissivity measurements by Cabannes et al. [83], Held and Wilder [84], and Schoenes [85] but disagree with the earlier data of Claudson [86]. Data in the range of 1000–3120 K indicate that the emissivity of both sintered and premelted solid UO_2 varies little with temperature and is only a weak function of wavelength. Thus, the constant total hemispherical emissivity of 0.85 ± 0.05, which was recommended by Harding et al. [2], is recommended. The equation given by Bober et al. [81] for the normal spectral emissivity of premelted solid UO_2 at the wavelength of 630 nm, which was recommended in the 1981 assessment [1], is recommended for wavelengths in the visible range:

for 1000 K $\leqslant T \leqslant$ 3120 K and 400 nm $\leqslant \lambda \leqslant$ 700 nm

$$\begin{aligned}&\varepsilon\ (\lambda = 630\ \text{nm})\\ &\quad = 0.836 + 4.321 \times 10^{-6}(T - 3120),\end{aligned} \tag{29}$$

where T is in K.

The emissivity of liquid UO_2 is a function of both wavelength and temperature. For wavelengths in the visible range, however, the normal spectral emissivity of liquid UO_2 is approximately independent of wavelength. The recommended values as a function of temperature for this wavelength range are those calculated from an equation for a wavelength of 630 nm determined by Fink [87]

for 3120 K $\leqslant T \leqslant$ 4200 K and 400 nm $\leqslant \lambda \leqslant$ 700 nm,

$$\varepsilon\ (\lambda = 630\ \text{nm}) = 1 - 0.16096\ \exp[-3.7897 \times 10^{-4}\Delta T - 3.2718 \times 10^{-7}(\Delta T)^2], \quad (30)$$

where $\Delta T = T - 3120$ K. Although Eq. (30) was derived to fit the data of Bober et al. [81] at a wavelength of 630 nm, it also gives a good fit to more recent data [16,17] at wavelengths of 548, 514.5, 647 and 752.5 nm. However, the behavior of the emissivity in the infrared region differs considerably from Eq. (30). Bober et al. [81] found that the normal spectral emissivity at a wavelength of 10 600 nm falls from 0.85 at 3120 K to 0.64 at 3670 K and to 0.4 at 4000 K. Further emissivity measurements of liquid UO_2 are needed in the infrared and far infrared region to confirm these results.

Bober et al. determined optical constants of single-crystal UO_2 at 300 K from reflectivity measurements in the spectral range of 450–750 nm. Ackermann et al. [88] determined the index of refraction at room temperature in the ultraviolet region (at the wavelength of 260 nm) and in the visible range (at wavelengths from 450 to 800 nm). Although values reported by Ackermann et al., are consistently higher than those given by Bober et al., they are within the estimated 10% experimental uncertainty given by Bober et al. The average values obtained by Bober et al for the index of refraction (n) and absorption coefficient (k) of UO_2 at 300 K are, respectively, 2.2 and 0.7.

Bober et al. [16,17] determined the optical constants for liquid UO_2 from reflectivity measurements with polarized light in the temperature range of 3000–4000 K at four visible wavelengths (458, 514.5, 647 and 752.5 nm) and at three angles of incidence (45°, 58° and 71°). Both optical constants decrease with increasing temperature. From their data, Bober et al., recommend an average value of 1.7 for the refractive index and 0.8 for the absorption coefficient for visible wavelengths in the temperature range from 3100 to 3600 K. However, because the reflectivities measured as a function of temperature and wavelength showed considerable scatter with angle of incidence, Bober et al. estimated large uncertainties in the calculated refractive index and absorption coefficient.

14. Summary and uncertainties

From analysis of the available data, equations and values have been recommended for the thermodynamic and transport properties of solid and liquid UO_2. To provide information on the reliability of these equations and property values, uncertainties have been determined as a function of temperature. Uncertainties for recommended property values of solid UO_2 are given in Table 5. Uncertainties for recommended equations for liquid properties are given in Table 6. These uncertainties have been determined from experimental uncertainties (when available), scatter in the data, deviations of the data from the recommended equations, differences between available equations in the literature, and estimates of errors arising from extrapolation beyond measurements. The last column in Tables 5 and 6 gives the main methods used to determine the uncertainties for each property.

From this assessment and the uncertainties in Tables 5 and 6, some conclusions may be made regarding needs for further thermophysical property measurements. The available data on the thermophysical properties of solid UO_2 appear to be adequate for reactor-safety calculations. However, independent confirmation of the recent thermal diffusivity and heat capacity data of Ronchi et al. [5] above 2000 K would be useful in reducing the uncertainties. Because of measurement difficulties and lack of calibration standards, properties of liquid UO_2 that are important for reactor-safety assessments still have large uncertainties. Data are needed on the temperature dependence of the liquid properties of surface tension, thermal conductivity and thermal diffusivity. Although the liquid heat capacity data of Ronchi et al. [6] and constant thermal conductivity of Tasman [10] imply that the thermal diffusivity increases slightly with temperature, the available thermal diffusivity measurements are inadequate to confirm this behavior. New thermal diffusivity measurements are needed that take into account corrections for radiation effects using optical constants that are now available. Because analysis of the heat capacity measurements included the assumption of a constant thermal conductivity, it is unclear if the heat capacity temperature dependence is correct. Enthalpy measurements are needed above 3500 K for a combined analysis with the heat capacity data to reduce the heat capacity uncertainties and to confirm the temperature dependence.

The equations for the thermophysical properties of UO_2 that are given in this paper are intended for stoichiometric uranium dioxide fuel and should not be used for the calculation of properties of high-burnup UO_2 fuel. Although extensive research has been done on material properties of high-burnup fuel and on simulated high-burnup UO_2 fuel (SIMFUEL), a complete review of that data is beyond the scope of this paper.

Table 5
Uncertainties for recommended properties of solid UO_2

Property	Temperature range (K)	Uncertainty (%)	Basis for uncertainty
Enthalpy, H	298–1800 1800–3120	±2 ±3	Scatter in data, deviation of data from recommended equation
Heat capacity, C_P	298–1800 1800–3120	±4 ±13	Scatter in data, deviation of data from recommended equation
Thermal expansion, $\Delta L/L$	537–1100 1100–3120	±10 ±7	Scatter in data, deviation of data from recommended equation
Density, ρ	298–3120	±1	Comparison with other recommended equations
Thermal conductivity, λ	298–2000 2000–3120	±10 ±20	Scatter in data, deviation of data from recommended equation
Surface energy, γ	273–3120	±70	Analysis of Hall et al. [71–73]
Emissivity, ε premelted UO_2	1000–1500	±1	Analysis of Bober et al. [81]
	1500–3120	±2	
Optical constants, n, k	300	±10	Estimated by Bober et al. [16,17] based on deviations from Ackermann's data

Table 6
Uncertainties for recommended properties of liquid UO_2

Property	Temperature range (K)	Uncertainty (%)	Basis for uncertainty
Enthalpy, H	3120–3500 3500–4500	±2 ±10	Deviation of data from recommended equation, deviation of equation from other equations. Above 3500 K, extrapolation beyond data
Heat capacity, C_P	3120–3400 3400–4500	±10 ±10–25	Scatter in data, deviation of data from recommended equation. Linear increase from 3400–4500 K
Density, ρ	3120–3500 3500–4500	±2 ±4	Experimental uncertainties of mass, volume, enthalpy, determined by Breitung and Reil [13]
Thermal conductivity, λ	3120	±40	Estimated by Tasman [10]; deviations from thermal diffusivity with radiative corrections
Vapor pressure, P	3120 4500	−40/+60 −42/+80	Estimated from scatter in data, assumed to increase linearly with temperature
Surface tension, γ	3120	±17	Standard deviation of average of 4 measurements
Viscosity, η	3120–3400 3400–4000	±25 ±50	Estimate based on lack of high-temperature standards. Extrapolation beyond data above 3400 K
Emissivity, ε	3120–4200	±3	Deviation of equation from data and experimental error given by Bober et al. [81,87]
Index of refraction, n	3120–3600	±10	Estimated by Bober et al. [16,17] from scatter in reflectivity data
Absorption coefficient, k	3120–3600	±20	Estimated by Bober et al. [16,17] from scatter in reflectivity data

To provide the reader with an idea of the magnitude of the effects of high burnups on thermophysical properties of fuel, the percent change of the properties of SIMFUEL that are most effected by burnup (density, heat capacity and thermal conductivity) from the values of these properties for UO_2 are summarized in Tables 7 and 8 as a function of burnup and oxgen to metal ratio (O/M).

Table 7 gives the decrease in room-temperature density with burnup from SIMFUEL data [89–92]. The effects of addition of fission products on the lattice parameters are discussed by Lucuta et al. [90]. A complete review of lattice parameter changes with burnup and oxidation has been given by Cobo et al. [94]. Although the initial density of the fuel is effected by burnup, as shown in Table 7, the change of density with temperature and thermal expansion are adequately represented by the thermal expansion of UO_2. From his review of thermal expansion data for UO_{2+x}, Martin [40] concluded that the thermal expansion of UO_{2+x} for $0 < x < 0.13$ and $0.235 < x < 0.25$ is virtually the same as that for $UO_{2.00}$ up to 1520 K and suggested that the temperature range may be extended to the melting point. Lucuta et al. [90] use the thermal expansion of UO_2 to account for the temperature variation of density of SIMFUEL.

Heat capacity measurements on UO_2-based SIMFUEL, shown in Table 7, indicate that the heat capacity increases with burnup and with increased oxygen potential. For burnups of 3% and 8% and an O/M of 2.00, the heat capacity increase of 1.5% is within the uncertainty given in Table 5. The heat capacities of SIMFUEL with burnups of 3% and 8% and O/M in the range of 2.03–2.07 have a hump between 400°C and 600°C caused by the U_4O_9 phase [92]. A similar hump is also seen in hypostoichiometric UO_{2+x} and in UO_2 that is contaminated with U_4O_9.

Effects of burnup and hypostoichiometry on the thermal conductivity of SIMFUEL have been extensively studied [93,95–97]. Table 8 shows data from Lucuta et al. [93] for two temperatures. For 3% burnup at temperatures of 1000 K or higher and for 8% burnup, these data are in good agreement with equations developed by Amaya and Hirai [96]. From their SIMFUEL data and available data on irradiated fuel, Lucuta et al. [97] have developed equations for the thermal conductivity of high-burnup fuel for normal operating condi-

Table 7
Percent changes of properties of high-burnup UO_2 from properties of UO_2

Property	Change (%)	Burnup (at.%)	O/M	Reference
Density, ρ (room temperature)	−1	3	2.00, 2.02	[89]
	−1.4	3	(Not given)	[90]
	−1.6	3	(Not given)	[91]
	−2	6	2.00, 2.02	[92]
	−3	6	(Not given)	[91]
	−3.6	8	(Not given)	[90]
Heat capacity, C_P (300–1700 K)	+1.5	3–8	2.00	[90]
	+2	0	2.04	[92]
	+3	3	2.07	[92]
	+5	0	2.08	[92]
	+6	8	2.03–2.07	[92]

Table 8
Percent changes of thermal conductivity of high-burnup UO_2 from UO_2 thermal conductivity [93]

T (K)	Burnup (at.%)	O/M			
		2.00	2.007	2.035	2.084
		Change from UO_2 (%)			
873	0	–	−15	−37	−56
	3	−20	−24	−37	−56
	8	−31	–	−41	−55
1773	0	–	−11	−23	−33
	3	−11	−14	−24	−32
	8	−18	–	−23	−31

tions up to 1900 K and for failed fuel that take into account the effects from fission products, deviation from stoichiometry, and radiation damage. For high-burnup fuel under normal operating conditions, their analytical expression includes factors describing these effects applied to the equation for unirradiated UO_2 thermal conductivity developed by Harding and Martin [20]. The deviation of the equation of Harding and Martin from the recommended thermal conductivity equation, Eq. (19) modified to 100% theoretical density, is 5% from 500 to 1500 K and less than the 10% uncertainty through 1900 K. Thus, Eq. (19) for 95% dense UO_2 corrected to theoretical density using Eq. (18), may be used in place of the equation of Harding and Martin in the analytical expression of Lucuta et al. [97] The conductivity formula for sintered, stoichiometric uranium dioxide proposed by Lucuta et al. [97] has been incorporated in the FRAPCON-3 code [98].

This paper has summarized new analyses and recommendations for the thermophysical properties of UO_2. Detailed summaries of the analyses, tabulated recommended values as a function of temperature, and comparisons with data and with previous analyses are available from the International Nuclear Safety Center Material Properties Database located on the World Wide Web at http://www.insc.anl.gov.

Acknowledgements

The technical comments from the peer review of the preliminary Argonne National Laboratory Report ANL/RE-97/2 by A.D. Efanov, I.P. Smogalev, and V.P. Bobkov from the State Scientific Center of the Russian Federation Institute of Physics and Power Engineering are greatly appreciated. The author thanks L. Leibowitz, and T.H. Bauer for their technical reviews of this paper. This work has been supported by the US Department of Energy under Contract W-31-109-ENG-38.

References

[1] J.K. Fink, M.G. Chasanov, L. Leibowitz, J. Nucl. Mater. 102 (1981) 17.
[2] J.H. Harding, D.G. Martin, P.E. Potter, Thermophysical and Thermochemical Properties of Fast Reactor Materials, Harwell Laboratory UKAEA Report EUR 12402, 1989.
[3] M.T. Hutchings, J. Chem. Soc. Farady Trans. II 83 (1987) 1083.
[4] J.P. Hiernaut, G.J. Hyland, C. Ronchi, Int. J. Thermophys. 14 (1993) 259.
[5] C. Ronchi, M. Sheindlin, M. Musella, G.J. Hyland, J. Appl. Phys. 85 (1999) 776.
[6] C. Ronchi, J.P. Hiernaut, R. Selfslag, G.J. Hyland, Nucl. Sci. Eng. 113 (1993) 1.
[7] A.C. Momin, E.B. Miza, M.D. Mathews, J. Nucl. Mater. 185 (1991) 308.
[8] C. Otter, D. Damien, High Temp. – High Press. 16 (1984) 1.
[9] H.A. Tasman, D. Pel, J. Richter, H.E. Schmidt, High Temp. – High Press. 15 (1983) 419.
[10] H.A. Tasman, Thermal Conductivity of Liquid UO_2, Commision of the European Communities Joint Research Centre Annual Report, Karlsruhe, Germany TUAR88, 1988.
[11] R. Limon, G. Sutren, P. Combetter, F. Barbry, in: Proceedings of the ENA/ANS Topical Meeting on Reactor Safety Aspects of Fuel Behavior, Sun Valley, Idaho, USA, 2–6 August 1981, CEA-CONF-5816, American Nuclear Society, 1981, vol. 2, p. 2-576.
[12] R.W. Ohse, J.F. Babelot, C. Cercignani, J.P. Hiernaut, M. Hoch, G.J. Hyland, J. Magill, J. Nucl. Mater. 130 (1985) 165.
[13] W. Breitung, K.O. Reil, Proc. of Conf. on Science and Technology of Fast Reactor Safety, Guernsey, UK, 12–16 May 1986, p. 501.
[14] W. Breitung, K.O. Reil, Kernforschungszentrum Karlsruhe, Germany Report KfK-3939, 1985.
[15] M. Bober, J. Singer, Nucl. Sci. Eng. 97 (1987) 344.
[16] M. Bober, J. Singer, K. Wagner, in: Proceedings of the Eighth Symposium on Thermophysical Properties, vol. II, Gaithersburg, MD, 1981, ASME, New York, 1982, p. 234.
[17] M. Bober, J. Singer, K. Wagner, J. Nucl. Mater. 124 (1984) 120.
[18] L.V. Matweev, M.S. Veshchunov, J. Nucl. Mater. 265 (1999) 285.
[19] G.J. Hyland, J. Nucl. Mater. 113 (1983) 125.
[20] J.H. Harding, D.J. Martin, J. Nucl. Mater 166 (1989) 166.
[21] J.K. Fink, L. Leibowitz, High Temp. – High Press. 17 (1985) 17.
[22] C.S. Kim, R.A. Haley, J. Fischer, M.G. Chasanov, L. Leibowitz, in: A. Cezairliyan (Ed.), Proceedings of the Seventh Symposium on Thermophysical Properties, ASME, New York, 1977, p. 338.
[23] J.K. Fink, M.C. Petri, Thermophysical Properties of Uranium Dioxide, Argonne National Laboratory Report ANL/RE-97/2, 1997.
[24] C. Ronchi, G.J. Hyland, J. Alloys Compounds 213/214 (1994) 159.
[25] J.K. Fink, Int. J. Thermophys. 3 (1982) 165.
[26] A.E. Ogard, J.A. Leary, in: Thermodynamics of Nuclear Materials 1967, IAEA, Vienna, 1969 p. 651.
[27] G.E. Moore, K.K. Kelly, J. Am. Chem. Soc. 69 (1947) 2105.
[28] D.R. Fredrickson, M.G. Chasanov, J. Chem. Thermo. 2 (1970) 263.
[29] R.A. Hein, L.A. Sjodahl, R. Szwarc, J. Nucl. Mater. 25 (1968) 99.
[30] R.A. Hein and P.N. Flagella, Enthalpy measurements of UO_2 and tungsten to 3260 K, General Electric Report GEMP-578, 1968.
[31] L. Leibowitz, L.W. Mishler, M.G. Chasanov, J. Nucl. Mater. 29 (1969) 356.
[32] J.J. Hunzicker, E.F. Westrum, J. Chem. Thermo. 3 (1971) 61.
[33] F. Gronvold, N.J. Kveseth, A. Sveen, J. Tichy, J. Chem. Thermo. 2 (1970) 665.

[34] C. Affortit, High Temp. – High Press. 1 (1969) 27.
[35] C. Affortit, J. Marcon, Rev. Int. Hautes Temp. Refract. 7 (1970) 236.
[36] M.M. Popov, G.L. Galchenko, M.D. Seniv, Zh. Neorg. Kim. 3 (1958) 1734 [English translation: J. Inorganic Chem. 3 (1958) 18].
[37] T.K. Engel, J. Nucl. Mater. 31 (1969) 211.
[38] P. Browning, G.J. Hyland, J. Ralph, High Temp. – High Press. 15 (1983) 169.
[39] M.H. Rand, R.J. Ackermann, F. Gronvold, F.L. Oetting, A. Pattoret, Rev. Int. Hautes Temp. Refract. 15 (1978) 355.
[40] D.G. Martin, J. Nucl. Mater. 152 (1988) 94.
[41] A.J. Christensen, J. Am. Ceram. Soc. 46 (1963) 607.
[42] J.B. Conway, R.M. Fincel, R.A. Hein, Trans. Am. Nucl. Soc. 6 (1963) 153.
[43] P.J. Baldock, W.E. Spindler, T.W. Baker, J. Nucl. Mater. 18 (1966) 305.
[44] W.A. Lambertson, J.H. Hanwerk, The fabrication and physical properties of urania bodies, Argonne National Laboratory Report ANL-5053, 1963.
[45] J.M. Leblanc, H. Andriessen, EURATOM/USA Report EURAEC-434, 1962.
[46] M.D. Burdick, H.S. Parker, J. Am. Ceram. Soc. 39 (1956) 181.
[47] N.H. Brett, L.E. Russell, in: E. Grison, W.B.H. Lord, R.D. Fowler (Eds.), Plutonium 1960, Cleaver Hyne Oress, London 1961, p. 397.
[48] M. Hoch, A.C. Momin, High Temp. – High Press. 1 (1969) 401.
[49] F. Gronvold, J. Inorg. Nucl. Chem. 1 (1955) 357.
[50] W. Breitung, K.O. Reil, Nucl. Sci. Eng. 105 (1990) 205.
[51] W.D. Drotning, in: Proceedings of the Eighth Symposium on Thermophysical Properties, Gaithersburg, MD, National Bureau of Standards 1981, 15–18 June 1981.
[52] J.C. Weilbacher, Measurement of thermal diffusivity of mixed uranium plutonium oxides, Centre d'etudes nucleairs de Fontenay-aux-Roses, France Report CEA-R-4572, 1974.
[53] J.C. Weilbacher, High Temp. – High Press. 4 (1972) 431.
[54] I.C. Hobson, R. Taylor, J.B. Ainscough, J. Phys. D 7 (1974) 1003.
[55] J. Lambert Bates, High-temperature thermal conductivity of round robin' uranium dioxide, Battelle Memorial Institute Pacific Northwest Laboratories Report BNWL-1431, 1970.
[56] J.B. Conway, A.D. Feith, An interim report on a round robin experimental program to measure the thermal conductivity of stoichiometric uranium dioxide, General Electric Report GEMP-715, 1969, also addendum, 1970.
[57] T.G. Godfrey, W. Fulkerson, T.G. Kollie, J.P. Moore, D.L. McElroy, The thermal conductivity of uranium dioxide and armco iron by an improved radial heat flow technique, Oak Ridge national Laboratory Report ORNL-3556, 1964.
[58] J.C. Stora, B. de Bernardy de Sigoyer, R. Delmas, P. Deschamps, B. Lavaud, C. Ringot, conductivilite thermique de l'UO2 frite dans les conditions d'utilisation en pile, Centre d'etudes nucleaires de Saclay France Report CEA-R-2586, 1964.
[59] J.M. Casado, J.H. Harding, G.J. Hyland, J. Phys.: Condens. Matter 6 (1994) 4685.
[60] J.C. Killeen, J. Nucl. Mater. 92 (1980) 136.
[61] R. Brandt, G. Neuer, J. Non-Equilib. Thermodyn. 1 (1976) 3.
[62] A.B.G. Washington, Preferred values for the thermal conductivity of sintered ceramic fuel for fast reactor use, UK Atomic Energy Authority TRG-Report -2236, 1973.
[63] M.F. Lyons, D.H. Coplin, T.J. Pashos, B. Weodembai,. General Electric Company Report GEAP-44624, 1964, as referenced by Ronchi et al. (Ref. 5).
[64] C. Ronchi, J. Phys.: Condens. Matter 6 (1994) L561.
[65] K.C. Mills, W.A. Wakeham, High Temp. – High Press. 17 (1985) 343.
[66] S. Fischer, E. Obermeier, High Temp. – High Press. 17 (1985) 699.
[67] W. Breitung, K.O. Reil, Nucl. Sci. Eng. 101 (1989) 26.
[68] D.W. Green, L. Leibowitz, J. Nucl. Mater. 105 (1982) 94.
[69] R.W. Ohse, J.F. Babelot, A. Frezzotti, K.A. Long, J. Magill, High Temp. – High Press. 12 (1980) 537.
[70] G.T. Reedy, M.G. Chasanov, J. Nucl. Mater. 42 (1972) 341.
[71] R.O.A. Hall, M.J. Mortimer, D.A. Mortimer, J. Nucl. Mater. 148 (1987) 237.
[72] R.O.A. Hall, M.J. Mortimer, D.A. Mortimer, J. Less-Common Met. 121 (1986) 341.
[73] R.O.A. Hall, M.J. Mortimer, J. Nucl. Mater. 137 (1985) 77.
[74] H. Schins, J. Nucl. Mater. 78 (1978) 215.
[75] J.A. Christensen, Battelle-Northwest Laboratory Report, Richland, WA, BNWL-SA-588884-A, 1966.
[76] J.L. Bates, C.E. McNeilly, J.J. Rasmussen, Mater. Sci. Res. 5 (1971) 11.
[77] O. Nikolopoulos, B. Schulz, J. Nucl. Mater. 82 (1979) 172.
[78] R.E. Woodley, J. Nucl. Mater. 50 (1974) 103.
[79] R. Palinski, Core melts – measurement of some thermophysical properties of liquid reactor materials at high temperatures, Commission of European Communities Joint Research Centre, Ispra Establishment, Italy Report EUR 7002 EN, 1980.
[80] H.C. Tsai, D.R. Olander, J. Nucl. Mater. 44 (1972) 83.
[81] M. Bober, H.U. Karow, K. Muller, High Temp. – High Press. 12 (1980) 161.
[82] M. Bober, High Temp. – High Press. 12 (1980) 297.
[83] F. Cabannes, J.P. Stora, J. Tsakiris, C.R. Acad. Sc. Paris B 264 (1967) 45.
[84] P.C. Held, D.R. Wilder, J. Am. Ceram. Soc. 52 (1969) 152.
[85] J. Schoenes, J. Appl. Phys. 49 (1978) 1463.
[86] T.T. Claudson, Emissivity Data for Uranium Dioxide, Report AW-55414 (Nov. 1958); see also pp. 196–197, in: J. Belle (Ed.), Uranium Dioxide Properties and Nuclear Applications, US AEC, 1961.
[87] C.L. Fink, private communication to the author.
[88] R.J. Ackermann, R.J. Thorn, G.H. Winslow, J. Opt. Soc. Am. 49 (1959) 1107.
[89] M. Amaya, M. Hirai, J. Nucl. Mater. 246 (1997) 158.
[90] P.G. Lucuta, Hj. Matzke, R.A. Verrrall, H.A. Tasman, J. Nucl. Mater. 188 (1992) 198.
[91] P.G. Lucuta, R.A. Verrrall, Hj. Matzke, B.J. Palmer, J. Nucl. Mater. 178 (1991) 48.
[92] Hj. Matzke, P.G. Lucuta, R.A. Verrrall, J. Henderson, J. Nucl. Mater. 247 (1997) 121.
[93] P.G. Lucuta, Hj. Matzke, R.A. Verrrall, J. Nucl. Mater. 223 (1995) 51.

[94] J. Cobos, D. Papaioannou, J. Spino, M. Coquerelle, J. Alloys Compounds 271–273 (1998) 610.
[95] P.G. Lucuta, Hj. Matzke, R.A. Verrrall, J. Nucl. Mater. 217 (1994) 279.
[96] M. Amaya, T. Kubo, Y. Korei, J. Nucl. Sci. Technol. 33 (1996) 636.
[97] P.G. Lucuta, Hj. Matzke, I.J. Hastings, J. Nucl. Mater. 232 (1996) 166.
[98] D.D. Lanning, C.E. Beyer, and C.L. Painter, FRAPCON-3: Modifications to Fuel Rod Material Properties and Performance Models for High-Burnup Application, NUREG/CR-6534, vol. 1, 1997.